Article:
Fuller, J orcid.org/0000-0001-8801-149X, Surtees, RA, Shaw, AB et al. (7 more authors) (2019) Hazara nairovirus elicits differential induction of apoptosis and nucleocapsid protein cleavage in mammalian and tick cells. The Journal of General Virology, 100 (3). pp. 392-402. ISSN 0022-1317

https://doi.org/10.1099/jgv.0.001211

Hazara nairovirus elicits differential induction of apoptosis and nucleocapsid protein cleavage in mammalian and tick cells

J. Fuller[1], R. A. Surtees[1*], A. B. Shaw[1], B. Álvarez-Rodríguez[1], G. S. Slack[3], T. A. Edwards[1,2], R. Hewson[3], J. N. Barr[1,2†]

[1]School of Molecular and Cellular Biology, University of Leeds, Leeds, LS2 9JT, United Kingdom

[2]Astbury Centre for Structural Molecular Biology, University of Leeds, Leeds, LS2 9JT, United Kingdom

[3]National Infection Service, Public Health England, Porton Down, Salisbury SP4 0JG, United Kingdom

[*]Current address: Centre for Biological Threats and Special Pathogens, Robert Koch Institute, Seestrasse 10, Berlin, 13353, Germany.

Keywords – Apoptosis, Hazara Virus, Tick Cells, Mammalian Cells, Caspase, Nucleocapsid Protein

Word Count: Abstract: 250; Main text 5031 (excluding references).

[†]To whom correspondence should be addressed Tel: +44 (0)113-3438069; E-mail: j.n.barr@leeds.ac.uk

ABSTRACT

The *Nairoviridae* family within the *Bunyavirales* order comprise tick-borne segmented negative sense RNA viruses that cause serious disease in a broad range of mammals, yet cause a latent and life-long infection of tick hosts. An important member of this family is Crimean-Congo haemorrhagic fever virus (CCHFV), which is responsible for serious human disease that results in case-fatality rates of up to 30%, and which exhibits the most geographically-broad distribution of any tick-borne virus. Here, we explored differences in the cellular response of both mammalian and tick cells to nairovirus infection using Hazara virus (HAZV), which is a close relative of CCHFV within the CCHFV serogroup. We showed HAZV infection of human-derived SW13 cells led to induction of apoptosis, evidenced by activation of cellular caspases 3, 7 and 9. This was followed by cleavage of the classical apoptosis marker poly ADP-ribose polymerase, as well as cellular genome fragmentation. In addition, we showed that the HAZV nucleocapsid (N) protein was abundantly cleaved by caspase 3 in these mammalian cells at a conserved DQVD motif exposed at the tip of its arm domain, and that cleaved HAZV-N was subsequently packaged into nascent virions. However, in stark contrast, we showed for the first time that nairovirus infection of cells of the tick vector failed to induce apoptosis, evidenced by undetectable levels of cleaved caspases, and lack of cleaved HAZV-N. Our findings reveal that nairoviruses elicit diametrically-opposed cellular responses in mammalian and tick cells, which may influence the infection outcome in the respective hosts.

INTRODUCTION

The *Bunyavirales* order is comprised of over 400 named viruses that each possess a segmented negative or ambisense sense, single stranded RNA (-ssRNA) genome. The order is divided into nine families; *Feraviridae*, *Fimoviridae*, *Hantaviridae*, *Jonviridae*, *Nairoviridae*, *Peribunyaviridae, Phasmaviridae*, *Phenuiviridae* and *Tospoviridae*, and members are responsible for infection and disease across a broad range of hosts including insects, animals, plants and humans. The bunyavirales responsible for human disease are classified within the *Nairoviridae*, *Hantaviridae*, *Phenuiviridae* and *Peribunyaviridae* families, and include notable human pathogens such as Rift Valley fever virus (RVFV), Ngari virus, Hantaan virus and Crimean-Congo haemorrhagic fever virus (CCHFV), each of which has been reported to cause fatal hemorrhagic fevers in humans. Many bunyavirales members are emerging viruses, for which disease-prevention strategies do not exist.

Hazara virus (HAZV) is a nairovirus, and is classified in the same serogroup as CCHFV on the basis of its serological reactivity and nucleotide sequence [1]. CCHFV is the causative agent of Crimean-Congo haemorrhagic fever (CCHF), a human disease that generally has case fatality rates between 20-30%, although these can be significantly higher in specific outbreaks, with no effective approved treatment or vaccination options available [2]–[4]. These factors have led to the classification of CCHFV as a Hazard Group 4 pathogen, requiring the highest containment level 4 (CL-4) laboratories for its growth. Both HAZV and CCHFV are arboviruses that infect ticks of the genus *Hyalomma,* and are transmitted to mammalian hosts through a tick bite or contact with contaminated blood or tissue [5], [6]. Studies exploring infection of multiple mammalian species including rats, guinea pigs and donkeys showed infection with either HAZV or CCHFV resulted in successful viral replication but no clinical manifestation of disease. Despite the high fatality rate associated with CCHFV infection in humans, only interferon receptor knockout mice and infant mice showed fatal clinical symptoms following both CCHFV and HAZV infections, with both viruses showing similar disease progression [7], [8]. Due to the inability of HAZV to cause clinical disease in humans, it is classified as a Hazard Group 2 pathogen, which facilitates its use as a model for studying CCHFV without the need to work in Containment Level 4 laboratory conditions.

The HAZV and CCHFV genomes consist of three -ssRNA genome segments, termed small (S), medium (M) and large (L) according to their relative sizes. These minimally encode the nucleoprotein (N), viral glycoproteins (Gn and Gc) and the viral RNA dependent RNA polymerase (RdRp), respectively. A critical role of N in the nairovirus replication cycle is to bind newly generated RNA replication products forming ribonucleoprotein (RNP) complexes that represent the template for viral transcription and replication [9], [10]. In addition, N from several nairoviruses has been reported to possess DNA endonuclease activity [11], although the functional consequence of this ability remains unclear. Nairovirus N proteins also exhibit

extensive structural homology with the N protein of Lassa virus (LASV), a member of the bi-segmented *Arenaviridae* family [12]. The demonstration that LASV N possesses potent RNA endonuclease activity and the ability to supress anti-viral innate immunity [13] raises the interesting possibility that such functions are also shared with the N proteins from the *Nairoviridae* family.

Apoptosis is a critical cell response that ensures maintenance of homeostasis in multicellular organisms. Also being involved in the cellular response to injury, it is mediated via the sequential activation of a family of cysteine proteases known as caspases [14]. Activation of caspases requires an initial intrinsic or extrinsic signal; extrinsic signals originate from the death receptors of the tumour necrosis factor family on the cell surface, whilst intrinsic activation is mediated by cytochrome C release from the mitochondria causing activation of the initiator caspase, caspase 3 [15], [16]. The final result of apoptosis activation is cell death via cleavage of host-proteins by the activated executioner caspases 7 and 9, therefore complex regulatory mechanisms exist to modulate the process [17]. In order to facilitate the completion of their replication cycles, many viruses have evolved strategies to both induce or conversely delay induction of apoptosis. These strategies are diverse, targeting multiple stages of both the extrinsic and intrinsic pathways. For viruses that delay apoptosis, examples include inhibition of the pro-apoptotic tumour-suppressor p53 by the DNA virus SV40 and the direct inhibition of effector caspases by baculovirus p35 protein, which following cleavage remains irreversibly bound to the active site of the caspase [18]. Conversely, for viruses that promote apoptosis, examples include the closely-related Bunyamwera virus (BUNV) via activation of interferon regulatory factor 3 (IRF-3) and its related signalling pathways, and Oropouche virus in response to viral protein expression [19], [20]. Despite activation of apoptosis, BUNV and La Crosse virus (LACV) also regulate the induction of apoptosis at the early stages of infection through expression of the non-structural protein of the S segment (NSs) [21]. Together these strategies demonstrate the extensive arsenal viruses employ to modulate the cellular response to support their replication and survival.

In this study, we show that HAZV infection induces apoptosis in mammalian cells, and that N acts as a substrate for caspase 3 cleavage within infected cells. We identify the site of this cleavage and uncover extensive differences in cleavage of HAZV-N between tick vector and mammalian host cells that could have implications on how HAZV and, by association, CCHFV, are able to develop persistent infections in tick cells and modulate the mammalian apoptotic response [22].

MATERIALS AND METHODS

Viruses and cells.

Hazara virus, strain JC280 was propagated in SW13 cells (derived from human adrenal cortex) and maintained in Dulbecco's modified Eagle medium (DMEM) (Sigma Aldrich) containing 10% fetal bovine serum (FBS) (Invitrogen), 100 U/mL penicillin and 100 μg/mL streptomycin at 37°C in a 5% CO_2 atmosphere. Tick-derived HAE/CTVM9 (*Hyalomma anatolicum anatolicum*) cells were maintained in L15 containing 20% FBS, 10% tryptose phosphate broth, 2 mM L-glutamine, 100 U/mL penicillin and 100 μg/mL streptomycin at 30°C

Transfection of protein encoding plasmids.

For expression of wild type HAZV-N and derived mutants, liposome-based transfections into SW13 cells were carried out according to the manufacturer's instructions using 4 μL lipofectamine 2000 (Thermofisher) per μg of plasmid DNA. In all experiments, 1.5 μg of plasmid DNA was used to transfect 10^5 cells. Cell lysates were harvested on ice using RIPA buffer (150 mM sodium chloride, 1.0% NP-40 alternative, 0.1% SDS, 50 mM Tris, pH 8.0) at the indicated time points post transfection.

Viral infection of mammalian and tick cells.

SW13 monolayers were infected with HAZV at the specified multiplicity of infection (MOI) in serum-free DMEM (SFM) at 37°C. After 1 hour, the inoculum was removed and cells washed in phosphate buffered saline (PBS), fresh DMEM containing 2.5% FBS, 100 U/mL penicillin and 100 μg/mL streptomycin was then applied for the duration of the infection. For comparison of HAZV infection and apoptosis induction in HAE/CTVM9 and SW13 cell lines, SW13 or HAE/CTVM9 cells were infected at an MOI of 0.001 in 25 cm^2 flasks. Due to differences in cell behaviour, HAE/CTVM9 cells were infected in suspension and SW13 cells were infected as a monolayer at the respective culture conditions previously mentioned. In both cell types, virus was not removed following infection and flasks were returned to incubators for culture at their indicated temperatures.

Virus purification.

HAZV was grown in SW13 cells and purified as previously described [23]. Briefly, SW13 cells were infected as described above and virus-containing media harvested 72 hours post infection. HAZV-containing media was then clarified via centrifugation at 4000 x g for 20 minutes then HAZV particles were purified by pelleting through a 30% sucrose cushion, and then pellets were resuspended in PBS (pH 7.3) containing 0.5 mM $MgCl_2$ and 20 mM $CaCl_2$

and pooled. Purity of HAZV particles was assessed by PAGE, followed by Coomassie staining (data not shown) and western blotting with HAZV-N antiserum.

Inhibition of caspase 3.

Z-FA-FMK (Santa Cruz Biotechnology) was selected to inhibit a broad spectrum of caspases. Z-FA-FMK was resuspended in DMSO to a concentration of 20 mM. Immediately prior to use, aliquots were thawed on ice and diluted in DMEM supplemented with 2.5% FBS to a working concentration of 20 μM or 40 μM. SW13 cells were seeded at 1 x 10^5 cells per well in a 12-well plate, 24 hours later cells were infected with HAZV at a MOI of 1 as described above. Following adsorption of HAZV to cell membranes, SFM containing HAZV was removed and replaced with DMEM containing 2.5% FBS and the indicated concentration of Z-FA-FMK. Whole cell lysates were harvested 24, 48 or 72 hours post-infection and analysed via western blot.

Determination of cell viability.

MTT (2-(4,5-Dimethylthiazol-2-yl)-2,5-diphenyltetrazolium bromide) assays were used to assess the cytotoxicity of Z-FA-ZMK treatments on SW13 cells. SW13 cells (1 x 10^4) were seeded in 96-well plates 24 hours prior to treatment with Z-FA-FMK. At 24, 48 or 72 hours after treatment, MTT assays were performed using the CellTiter96 non-radioactive cell proliferation assay kit (Promega), according to the manufacturer's instruction. A dye solution containing MTT was added directly to the cells in 96 well plates, cells were incubated at 37°C for 4 hours, prior to addition of stop solution to solubilise the formazan product. Following overnight incubation, absorbance at 570 nm was recorded with the TECAN infinite F50 plate reader. Toxicity arising from DMSO at 0.1% or 0.2% dilutions was also compared; in both cases cell viability did not differ from untreated cells.

Transient expression of viral proteins in mammalian cells.

pCAGGS-HAZV-N was used as the template for site directed mutagenesis. Generation of mutant HAZV-N (D272A) was achieved using the Q5 Site Directed Mutagenesis kit (New England Biolabs) according to the manufacturer's instructions. The D272A mutant plasmid was validated via Sanger sequencing (GeneWiz).

Bacterial expression and digestion of recombinant proteins.

Recombinant CCHFV and HAZV-N proteins were expressed in bacterial cells and purified as previously described [12], [24]. Recombinant caspase 3 was expressed from a plasmid encoding the full-length protein fused to a C-terminal 6×His tag (pET21b-Caspase-3,

Addgene). Briefly, protein expression was induced in *E.coli* strain Rosetta 2 using 200 µM isopropyl β-D-1-thiogalactopyranoside (IPTG) at 30 °C for 4 hours. Cells were harvested by centrifugation and proteins were extracted by resuspension in lysis buffer (50 mM Tris-HCl pH 8, 100 mM NaCl, 1% Triton X-100, 1 mg/mL lysozyme (Sigma Aldrich), 1 unit (U) DNase and 1 U RNase). Lysates were clarified by centrifugation at 18,000 x g for 30 min at 4 °C and the supernatant was applied to Ni^{2+}-NTA resin pre-equilibrated in binding buffer (100 mM NaCl, 50 mM Tris-HCl pH 8.0, 20 mM imidazole). The unbound fraction was collected and the resin was washed in binding buffer and washing buffer (500 mM NaCl, 50 mM Tris-HCl pH 8.0, 50 mM imidazole). Elution buffer (100 mM NaCl, 50 mM Tris-HCl pH 8.0, 200 mM imidazole) was used to dissociate 6xHis-caspase 3 from the resin, and fractions containing purified caspase 3 were pooled and concentrated to 1 mg/mL.

Western blot analysis.

For preparation of cell lysates, monolayers were washed in ice cold PBS followed by incubation in ice cold RIPA buffer (150 mM sodium chloride, 1.0% NP-40 alternative, 0.1% SDS, 50 mM Tris, pH 8.0) and agitated for 120 seconds. Cells were then harvested via cell scraping and transferred to pre-chilled Eppendorf tubes, after which lysates were centrifuged at 20,000 x g for 15 minutes to pellet insoluble material. SDS-gel loading buffer containing DTT was added to the supernatant prior to storage at -20^{o}C. Proteins were separated on 12% SDS polyacrylamide gels by electrophoresis and transferred to fluorescence compatible PVDF (FL-PVDF) membranes. Sheep HAZV-N antiserum generated as previously described [25] was used to detect HAZV-N, and was subsequently visualised using fluorescently labelled anti-sheep secondary antibodies. For the detection of cellular markers of apoptosis, membranes were probed with primary antibodies against caspase 3, 7, 9 and poly ADP-ribose polymerase (PARP; Cell Signalling Technologies), and their respective cleaved forms (Cell Signalling Technologies) prior to the addition of the appropriate secondary antibodies. Membranes were visualised on the LiCor Odyssey Sa Infrared imaging system.

TUNEL assay.

Apoptosis and subsequent DNA fragmentation was detected with an *In-Situ* Cell Death Detection Kit, Fluorescein (Roche) according to the manufacturer's instructions. SW13 cells were seeded onto glass coverslips in 6 well plates 24 hours pre-infection, after which cells were infected with HAZV at a MOI of 1, or mock infected. Cells were fixed in 4% paraformaldehyde (PFA) at 24, 48 or 72 hours post-infection, and then permeabilised in 0.1% Triton-X 100 diluted in 0.1% sodium citrate for 5 minutes on ice. DNA strand breaks were then identified by labelling free 3'-OH DNA ends using the *In-Situ* Death Detection Kit, Fluorescein (Roche), in which the enzyme terminal deoxynucleotidyl transferase (TdT) catalyzed the

addition of fluorescently labelled nucleotides to free 3'-OH ends of cleaved DNA in a template independent manner. Cells were incubated with the enzyme reaction mix for 1 hour at 37°C. Fluorescein labelled nucleotides incorporated into nucleotide polymers were detected by fluorescence microscopy using the upright LSM 510 META confocal microscope (Carl Zeiss Ltd).

Results

HAZV induces apoptosis in mammalian cells.

The induction of apoptosis in mammalian cells has previously been described for the highly pathogenic nairovirus CCHFV, via both intrinsic and extrinsic pathways, and which was reported to be mediated by the CCHFV-NSs protein [26]. In order to determine whether the closely related HAZV also induced apoptosis in the mammalian SW13 cell line, SW13 cells were infected with HAZV at an MOI of 1 alongside a mock infected control. At 24, 48 and 72 hours post infection, cell lysates were harvested and analysed for the presence of native caspase 3, 7, 9 and PARP, as well as the corresponding cleaved forms that represent markers of apoptosis induction (Fig 1A). All full-length caspases and PARP were detected with similar abundance in both mock and HAZV-infected cell lysates at all time points tested, whereas cleaved forms of caspase 3, 7, 9 and PARP were detected in robust abundance at both 48 and 72 hours post infection in HAZV infected cells, indicative of apoptosis induction. In contrast, the cleaved forms were either undetectable or present at very low levels within mock infected cell cultures at all time points tested, indicating caspase cleavage and apoptosis was an infection-mediated response.

Alongside cleavage of caspases and their targets, we examined the effect of HAZV infection on an alternate marker of apoptosis, DNA fragmentation, via terminal dUTP nick end labelling (TUNEL) assay (Fig 1B). The TUNEL assay involves the enzymatic attachment of fluorescently labelled nucleotides to exposed 3' hydroxyl groups, that are abundant when the DNA is fragmented [27], resulting in increased punctate fluorescence that can be observed by fluorescence microscopy. Consistent with caspase induction (Fig 1A), HAZV infection of SW13 cells at both 48 and 72 hours post infection resulted in an increased abundance of punctate fluorescence (Fig 1B). Quantification at the 72-hour time point revealed approximately 20% of cells displayed DNA fragmentation versus less than 5% in mock infected cells. Taken together, these data show HAZV triggers apoptosis in mammalian cells at an early time point, after 24 hrs but before 48 hours post infection.

HAZV-N is cleaved in mammalian cells.

Previously, we and others have shown that nairoviruses possess conserved caspase cleavage sites within their respective N proteins [11], [12]. The N protein of CCHFV possesses an exposed DEVD motif that is recognised by caspase 3, and which has been suggested to be cleaved in a pro-cellular response, preserving cell viability and modulating infection. In addition, the presence of multiple caspase cleavage sites on the Junin arenavirus N protein was shown to delay apoptosis, possibly by acting as a substrate 'sink' to divert caspase-activation of downstream effectors [28].

The HAZV-N protein possesses a conserved DQVD motif in precise structural alignment with the DEVD sequence of the CCHFV N protein, which represents a potential substrate for cleavage by several caspases. Having established that HAZV infection of SW13 mammalian cells induces a robust apoptotic response, we next examined the interplay between apoptosis, activated caspases and the conserved DQVD motif within the HAZV-N protein during infection.

The expression and integrity of HAZV-N was investigated in SW13 cells following infection with HAZV at 24, 48 and 72 hour time points post infection by western blot analysis using HAZV-N antisera (Fig 2A). Multiple HAZV-N specific bands were observed at all time points tested and comprised full length HAZV-N at ≈54 kDa, as well as cleavage products at ≈45 kDa, ≈30 kDa and ≈20 kDa. At the 24 hour time point, bands representing full-length and 45 kDa N-specific forms were most abundant, whereas at the later 48 and 72 hour time points, bands corresponding to ≈30 kDa and ≈20 kDa forms were more readily detected. To determine whether these cleavage products were incorporated into virions, purified HAZV was analysed via western blotting for HAZV-N specific products (Fig 2B), which revealed both ≈30 kDa and ≈20 kDa cleaved forms were present, alongside multiple N-specific forms with molecular masses in the 45 kDa range. To predict the corresponding sites of possible cleavage, we utilised the GraBCas programme, which predicts recognition sites for caspases 1–9 and granzyme B within any given amino acid sequence. This resulted in the identification of potential cleavage motifs, ^{57}NERD^{60}, ^{248}DVMD^{251} and ^{269}DQVD^{272} (Fig 2C). Utilising the Expasy prediction tool, cleavage at the ^{269}DQVD^{272} site would generate products with estimated molecular masses of 30.7 kDa and 23.5 kDa, closely matching the products observed via western blot analysis (Fig 2A and B). In order to visualise the location of the cleavage site, the ^{269}DQVD^{272} motif is shown in relation to the 3D structural model and 2D schematic of HAZV-N (Fig 2D and E).

HAZV-N cleavage is abrogated by broad spectrum caspase inhibition.

To confirm the N protein cleavage products detected in cells (Fig 2) were caspase dependant, HAZV-infected SW13 cells were treated with the broad-spectrum caspase inhibitor Z-FA-FMK at concentrations of 20 μM or 40 μM, or cells were treated with DMSO as a control. Z-FA-FMK is an irreversible cysteine protease inhibitor that resembles the cleavage sites of known caspase substrates, functioning via alkylation of the critical cysteine residues in the caspase active site [29]. Western blot analysis of inhibitor treated cell lysates revealed a dramatic reduction in abundance of the ≈20 kDa HAZV-N fragment versus DMSO only controls (Fig 3A-C), indicating Z-FA-FMK treatment blocked N cleavage, and thus implicating the cleavage event as being caspase dependent. To rule out any effects on cell viability by Z-FA-

FMK, an MTT assay was performed (Fig 3D). Whilst cell viability levels were approximately 80% when treated with inhibitor versus the DMSO controls, there was no significant difference between the 20 μM or 40 μM doses, indicating the small effect on viability was not dose-dependent.

Mutations to the DQVD motif of HAZV-N prevent cleavage.

Having shown that HAZV-N within infected SW13 cells was cleaved by caspases to yield prominent ≈20 kDa and ≈30 kDa fragments, we next wanted to precisely identify the cleavage site. The DQVD (269-272) sequence within HAZV-N is located at a structurally identical site to the confirmed DEVD caspase 3 cleavage motif of CCHFV-N, strongly implicating this sequence as the target for cleavage. In addition, as mentioned above, cleavage at this DQVD site was predicted to yield the observed ≈ 20 kDa and ≈ 30 kDa species (Fig 2A).

To investigate whether the DQVD motif was the site of caspase cleavage, both wild-type (WT) and D272A forms of HAZV-N were transiently expressed from plasmids in SW13 cells undergoing apoptosis. The HAZV-N DQVD motif was modified by alanine substitution of the essential terminal D272 to generate an uncleavable DQVA sequence (HAZV-N-D272A). Cells expressing either HAZV-N or HAZV-N-D272A were treated at 24 hours post transfection with 1 μM staurosporine (STS) for 4 hours to induce apoptosis, after which cell lysates were collected and analyzed by western blot. As expected, transient expression of WT and mutant HAZV-N in all cells resulted in abundant detection of the 54 kDa full-length N (Fig 4A, blot panel 1). The presence of full-length caspase 3 was detected in all cell lysates (Fig 4A, blot panel 2), with cleaved caspase 3 only present in staurosporine treated cells (Fig 4A, blot panel 3), indicating that STS treatment has successfully triggered the induction of apoptosis. Crucially, in these apoptotic cells, the ≈20 kDa and ≈30 kDa cleaved forms of N were detected in cells expressing WT HAZV-N (Fig 4A, blot 4 and 5), and were almost undetectable in cells expressing mutant HAZV-N D272A (Fig 4A). Taken together these observations indicate cleavage at the DQVD site results in the observed HAZV-N-specific ≈20 kDa and ≈30 kDa products.

In this STS experiment, we used the detection of caspase 3 and its cleaved derivative solely as a marker for apoptosis induction. However, we previously demonstrated that CCHFV-N is a substrate for caspase 3 resulting in cleavage at its DEVD motif (Fig 4B), and work by others has shown that HAZV-N can also be cleaved by caspase 3, to apparently yield multiple products in the 20-30 kDa range [11]. To clarify the origin of these species, we next wanted to examine the caspase 3 cleavage profile of HAZV-N and confirm the identity of the resulting products by western blotting using HAZV-N antisera.

Recombinant bacterially-expressed CCHFV-N and HAZV-N proteins were incubated overnight with bacterially-expressed caspase 3 in either equimolar 1:1, or 2:1 ratios of caspase 3 to HAZV-N (Fig 4C and D). The resulting products of digestion were separated by SDS-PAGE and identified by western blotting using HAZV or CCHFV antisera, respectively, as well as cleaved caspase 3 antisera to confirm expression of the active protease. Caspase 3-mediated cleavage of both nairovirus N proteins was incomplete, with abundant full-length protein remaining, and the proportions of full-length and cleaved forms of HAZV-N were broadly similar. The HAZV-N blots revealed the presence of two prominent N protein cleavage products having approximate molecular masses of ≈20 kDa and ≈30 kDa, which corresponded precisely to the apparent masses of the HAZN-N products identified in apoptotic SW13 cells (Fig 2A). Taken together, these data show the ≈20 kDa and ≈30 kDa fragments seen in HAZV infected cells are caspase 3 generated.

Apoptosis and cleavage of HAZV-N is not observed in tick cells.

Nairoviruses such as CCHFV and HAZV are arboviruses that persist in life-long latent infections of their Hyalomma tick host, which contrasts sharply with the acute outcome of infection in human hosts, and is indicative of radically different host-pathogen interactions in these different cellular environments. In order to further explore these differences, HAZV infection of the tick cell line, HAE/CTVM9 was examined for its ability to support virus replication and induce apoptosis, as previously shown in SW13 cells (Fig 1A and B). Tick cells and SW13 cells were infected with HAZV and cell lysates were examined for expression of HAZV-N (Fig 5A and B) caspases 3, 7 and 9, as well as PARP in both their native and cleaved forms, 24, 48, 72 and 96 hours after infection by western blot analysis (Fig 5C). As with the mammalian SW13 cell line, initiator, executioner, or executioner targets (PARP) were abundantly expressed in tick cells at all time points. However, in stark contrast, the cleaved derivatives of all caspases and PARP were not detected, indicating that apoptosis was not induced in the tick-derived HAE/CTVM9 cell line at the time points tested.

Consistent with this finding, and the identification of the DQVD caspase 3 cleavage site in HAZV-N (Fig 4), the ≈20 kDa and ≈30 kDa caspase cleavage products of HAZV-N were either absent or detected in very low abundance in the HAE/CTVM9 cells (Fig 5B) indicating that HAZV-N remains mostly uncleaved in tick cells. These findings emphasize the differences between arthropod and mammalian cellular environments that are characterized by significantly different processing of virally encoded proteins.

DISCUSSION

The life-cycle of HAZV and CCHFV nairoviruses exists in an enzootic cycle between ticks of the *Hyalomma* genus and mammals, yet despite discovery of CCHFV in 1944, little is known about the life-cycle of nairoviruses in cells of the natural tick host [30]. Current understanding suggests these viruses are able to form persistent, life-long infections, with no apparent detrimental effects on the tick vector, compared to transient and acute infections in their mammalian hosts [31] suggesting radical differences in these respective host-pathogen interactions.

Here we revealed one such difference, which is the ability of HAZV to induce apoptosis with the subsequent cleavage of HAZV-N in mammalian cells, in stark contrast to the lack of apoptosis induction and N cleavage in tick cells. The closely related CCHFV has previously been shown to induce apoptosis in mammalian cells at 18 hours post infection, via significant increases in mitochondrial associated apoptotic mediators such as BAX and XBP1s, with the response increasing through 24 and 48 hours [32]. This induction was subsequently shown to be stimulated through expression of a possible NSs accessory protein expressed by ambisense transcription from a second open reading frame (ORF) within the S segment. Here, we showed that HAZV infection of human SW13 cells led to induction of apoptosis between 24-48 hours, suggesting this cellular response is a consistent feature of nairovirus multiplication in mammalian cells. Whether HAZV induces apoptosis by a functionally analogous S segment encoded protein is not yet known, although a second ORF does exist in a similar location to the NSs ORF of CCHFV [33]. In the case of CCHFV replication, the use of caspase inhibitors to block apoptosis induction resulted in a modest increase in virus titres, leading to the suggestion that apoptosis was a pro-cellular response that resulted in the restriction of virus growth. This suggestion raises several interesting questions, such as why does CCHFV express a pro-apoptotic protein that subsequently reduces virus titres, and clearly more work remains to be done to resolve these fundamental questions. One possibility is that the function of innate immune regulating components, such as the above mentioned NSs protein, is confined to one or other of the natural hosts, rather than both, by differential ability to interact with a respective host factor. Our observation that HAZV infection of tick cells in culture does not induce apoptosis may directly relate to the ability of the virus to establish persistent infections in the tick host. It could be that HAZV possesses the ability to delay or prevent apoptosis induction in the tick cell, but may be ineffective in preventing apoptosis induction in mammalian cells due to differences in effector host components.

La Crosse virus (LACV), for example, is another arbovirus of the *Bunyavirales* order, which infects both mammalian and insect hosts, however the outcome of these infections are extremely different; whilst mammalian cells display extensive cytopathic effects as a result of the inhibition of the anti-apoptotic properties of heat shock chaperone 70 [34], infection in

mosquito cells is not cytopathic and leads to persistence [35]. This difference in infection outcome in vector and host cells is also mirrored in BUNV infections, where cytopathic effects are detectable by 36 hours post infection in mammalian cell lines, whereas persistent, non-cytopathic infections are established in mosquito cells [36].

A further interesting aspect of nairovirus apoptosis induction is the cleavage of the N protein, which we previously showed occurred *in vitro* at a conserved site on the exposed tip of the CCHFV-N arm domain [12]. Here we show a similar caspase cleavage event occurs at the equivalent site on HAZV-N during mammalian cell infection.

It remains to be determined what role the cleavage of HAZV-N by cellular caspases might play in the replication cycle of HAZV. In the case of influenza virus, caspase cleavage of its functionally analogous N appears to be required for infection, as evidenced by the finding that viruses bearing caspase site alterations cannot be rescued into infectious viruses [37]. In the case of Junin arenavirus (JUNV), the functionally-analogous N protein possesses multiple caspase cleavage sites that are thought to act as decoy caspase 3 substrates, thereby interfering with activation of downstream executioner caspases, and delaying apoptosis induction [28]. This conclusion is consistent with the high conservation of these JUNV caspase recognition motifs, which interestingly, is also a feature of the nairovirus N. In the face of the high mutation rate of RNA viruses, we believe the conservation of these cleavage sites is highly suggestive of a pro-viral role, although what this role might be is currently unknown. Previous work has shown that alteration of the caspase cleavage site in CCHFV-N increases RNA synthesis, indicating the role of this cleavage may be at an alternative stage of the virus life-cycle [38]. It is also worth noting that the cleavage site of HAZV-N lies at the critical interface between monomers when they are in an oligomerised state, and alterations to this motif may have structural impacts in addition to loss of the cleavage site [24]. In contrast to the outcome of infection in mammalian cells, we showed that HAZV infection in tick cells was not associated with substantial N cleavage. This is an important finding as it suggests that such cleavage events are not obligatory for completion of the many roles of N in the HAZV infectious cycle, such as RNP assembly, RNA synthesis, segment packaging and virion assembly. Further analysis of the role of the conserved DQVD motif, and N caspase cleavage will be facilitated by the development of a reverse genetics system for HAZV, to complement the system already available for CCHFV.

ACKNOWLEDGEMENTS

The authors would like to thank Dr Bell-Sakyi and the Tick Cell Biobank, University of Liverpool for kindly providing HAE/CTVM9 cells.

AUTHOR CONTRIBUTIONS

Author contributions are as follows: JF, RAS, ABS, BA-R, GS, RH and JNB conceptualized the study; JF, RAS, ABS, BA-R, GS performed the experimental investigation; JF, RAS and JNB wrote the original draft manuscript; ABS, BA-R, GS reviewed and edited the manuscript; TAE, RH and JNB supervised the core team; JNB provided management and coordination of the research activities and acquired the financial support for the project.

CONFLICTS OF INTEREST

The author(s) declare that there are no conflicts of interest

FUNDING

This work was funded by a Public Health England (PHE) PhD studentship (to J. Fuller), EU Marie Skłodowska-Curie Actions (MSCA) Innovative Training Networks (ITN): H2020-MSCA-ITN-2016, grant agreement No 721367 (to B. Álvarez-Rodríguez) and Biotechnology and Biological Sciences Research Council (BBSRC) PhD studentship to A. B. Shaw.

REFERENCES

[1] L. Lasecka and M. D. Baron, “The molecular biology of nairoviruses, an emerging group of tick-borne arboviruses,” *Arch. Virol.*, vol. 159, no. 6, pp. 1249–1265, 2014.

[2] S. K. Al-Tikriti, F. Al-Ani, F. J. Jurji, H. Tantawi, M. Al-Moslih, N. Al-Janabi, M. I. Mahmud, A. Al-Bana, H. Habib, H. Al-Munthri, S. Al-Janabi, K. AL-Jawahry, M. Yonan, F. Hassan, and D. I. Simpson, “Congo/Crimean haemorrhagic fever in Iraq,” *Bull. World Health Organ.*, vol. 59, no. 1, pp. 85–90, 1981.

[3] A. Papa, I. Christova, E. Papadimitriou, and A. Antoniadis, “Crimean-Congo hemorrhagic fever in Bulgaria,” *Emerg. Infect. Dis.*, vol. 10, no. 8, pp. 1465–1467, 2004.

[4] P. Nabeth, D. O. Cheikh, B. Lo, O. Faye, I. O. M. Vall, M. Niang, B. Wague, D. Diop, M. Diallo, B. Diallo, O. M. Diop, and F. Simon, “Crimean-Congo hemorrhagic fever, Mauritania,” *Emerg. Infect. Dis.*, vol. 10, no. 12, pp. 2143–2149, 2004.

[5] F. Begum, C. L. Wisseman, and J. Casals, “Tick-borne viruses of west pakistan: II. Hazara virus, a new agent isolated from Ixodes redikorzeviticks from the Kaghan Valley, W. Pakistan,” *Am. J. Epidemiol.*, vol. 92, no. 3, pp. 192–194, 1970.

[6] T. G. Okorie, “Comparative studies on the vector capacity of the different stages of Amblyomma variegatum Fabricius and Hyalomma rufipes Koch for Congo virus, after intracoelomic inoculation,” *Vet. Parasitol.*, vol. 38, no. 2–3, pp. 215–223, 1991.

[7] S. E. Smirnova, “A comparative study of the Crimean hemorrhagic fever-Congo group of viruses,” *Arch. Virol.*, vol. 62, no. 2, pp. 137–143, 1979.

[8] S. D. Dowall, S. Findlay-Wilson, E. Rayner, G. Pearson, J. Pickersgill, A. Rule, N. Merredew, H. Smith, J. Chamberlain, and R. Hewson, “Hazara virus infection is lethal for adult type I interferon receptor-knockout mice and may act as a surrogate for infection with the human-pathogenic Crimean-Congo hemorrhagic fever virus,” *J. Gen. Virol.*, vol. 93, no. 3, pp. 560–564, 2012.

[9] C. A. Whitehouse, “Crimean-Congo hemorrhagic fever,” *Antiviral Res.*, vol. 64, no. 3, pp. 145–160, 2004.

[10] S. Morikawa, M. Saijo, and I. Kurane, “Recent progress in molecular biology of Crimean-Congo hemorrhagic fever,” *Comp. Immunol. Microbiol. Infect. Dis.*, vol. 30, no. 5–6, pp. 375–389, 2007.

[11] W. Wang, X. Liu, X. Wang, H. Dong, C. Ma, J. Wang, B. Liu, Y. Mao, Y. Wang, T. Li, C. Yang, and Y. Guo, “Structural and Functional Diversity of Nairovirus-Encoded Nucleoproteins,” *J. Virol.*, vol. 89, no. 23, pp. 11740–11749, 2015.

[12] S. D. Carter, R. Surtees, C. T. Walter, A. Ariza, É. Bergeron, S. T. Nichol, J. A. Hiscox, T. A. Edwards, and J. N. Barr, “Structure, function, and evolution of the Crimean-Congo hemorrhagic fever virus nucleocapsid protein.,” *J. Virol.*, vol. 86, no. 20, pp. 10914–10923, 2012.

[13] X. Qi, S. Lan, W. Wang, L. M. L. Schelde, H. Dong, G. D. Wallat, H. Ly, Y. Liang, and C. Dong, “Cap binding and immune evasion revealed by Lassa nucleoprotein structure,” *Nature*, vol. 468, no. 7325, pp. 779–783, 2010.

[14] S. Elmore, “Apoptosis: A Review of Programmed Cell Death,” *Toxicol. Pathol.*, vol. 35, no. 4, pp. 495–516, 2007.

[15] A. Ashkenazi and V. M. Dixit, “Death receptors: signaling and modulation.,” *Science*, vol. 281, no. 5381, pp. 1305–1308, 1998.

[16] P. K. Ho and C. J. Hawkins, “Mammalian initiator apoptotic caspases,” *FEBS J.*, vol. 272, no. 21, pp. 5436–5453, 2005.

[17] B. J. Thomson, “Viruses and apoptosis,” *Int. J. Exp. Pathol.*, vol. 82, no. 2, pp. 65–76, 2001.

[18] Q. Zhou, J. F. Krebs, S. J. Snipas, A. Price, E. S. Alnemri, K. J. Tomaselli, and G. S. Salvesen, “Interaction of the baculovirus anti-apoptotic protein p35 with caspases. Specificity, kinetics, and characterization of the caspase/p35 complex,” *Biochemistry*, vol. 37, no. 30, pp. 10757–10765, 1998.

[19] A. Kohl, R. F. Clayton, F. Weber, A. Bridgen, R. E. Randall, and R. M. Elliott, “Bunyamwera Virus Nonstructural Protein NSs Counteracts Interferon Regulatory Factor 3-Mediated Induction of Early Cell Death,” *J. Virol.*, vol. 77, no. 14, pp. 7999–8008, 2003.

[20] G. O. Acrani, R. Gomes, J. L. Proença-Módena, A. F. da Silva, P. Oliveira Carminati,

M. L. Silva, R. I. M. Santos, and E. Arruda, “Apoptosis induced by Oropouche virus infection in HeLa cells is dependent on virus protein expression,” *Virus Res.*, vol. 468, no. 7325, pp. 779–783, 2010.

[21] G. Blakqori, S. Delhaye, M. Habjan, C. D. Blair, I. Sanchez-Vargas, K. E. Olson, G. Attarzadeh-Yazdi, R. Fragkoudis, A. Kohl, U. Kalinke, S. Weiss, T. Michiels, P. Staeheli, and F. Weber, “La Crosse Bunyavirus Nonstructural Protein NSs Serves To Suppress the Type I Interferon System of Mammalian Hosts,” *J. Virol.*, vol. 81, no. 10, pp. 4991–4999, 2007.

[22] L. Bell-Sakyi, “Continuous cell lines from the tick Hyalomma anatolicum anatolicum,” *J. Parasitol.*, vol. 77, no. 6, pp. 1006–1008, 1991.

[23] E. K. Punch, S. Hover, H. T. W. Blest, J. Fuller, R. Hewson, J. Fontana, J. Mankouri, and J. N. Barr, “Potassium is a trigger for conformational change in the fusion spike of an enveloped RNA virus,” *J. Biol. Chem.*, vol. 293, no. 26, 2018.

[24] R. Surtees, A. Ariza, E. K. Punch, C. H. Trinh, S. D. Dowall, R. Hewson, J. A. Hiscox, J. N. Barr, and T. A. Edwards, “The crystal structure of the Hazara virus nucleocapsid protein,” *BMC Struct. Biol.*, vol. 15, p. 24, 2015.

[25] R. Surtees, S. D. Dowall, A. Shaw, S. Armstrong, R. Hewson, M. W. Carroll, J. Mankouri, T. A. Edwards, J. A. Hiscox, and J. N. Barr, “Heat Shock Protein 70 Family Members Interact with Crimean-Congo Hemorrhagic Fever Virus and Hazara Virus Nucleocapsid Proteins and Perform a Functional Role in the Nairovirus Replication Cycle,” *J. Virol.*, vol. 90, no. 20, pp. 9305–9316, 2016.

[26] B. Barnwal, H. Karlberg, A. Mirazimi, and Y.-J. Tan, “The Non-structural Protein of Crimean-Congo Hemorrhagic Fever Virus Disrupts the Mitochondrial Membrane Potential and Induces Apoptosis,” *J. Biol. Chem.*, vol. 291, no. 2, pp. 582–592, 2016.

[27] K. Kyrylkova, S. Kyryachenko, M. Leid, and C. Kioussi, “Detection of apoptosis by TUNEL assay.,” *Methods Mol. Biol.*, vol. 887, pp. 41–47, 2012.

[28] S. Wolff, S. Becker, and A. Groseth, “Cleavage of the Junin Virus Nucleoprotein Serves a Decoy Function To Inhibit the Induction of Apoptosis during Infection,” *J. Virol.*, vol. 87, no. 1, pp. 224–233, 2013.

[29] P. Schotte, W. Declercq, S. Van Huffel, P. Vandenabeele, and R. Beyaert, “Non-specific effects of methyl ketone peptide inhibitors of caspases,” *FEBS Lett.*, vol. 442, no. 1, pp. 117–121, 1999.

[30] H. Hoogstraal, “The epidemiology of tick-borne Crimean-Congo hemorrhagic fever in Asia, Europe, and Africa.,” *J. Med. Entomol.*, vol. 15, no. 4, pp. 307–417, 1979.

[31] A. Papa, K. Tsergouli, K. Tsioka, and A. Mirazimi, “Crimean-Congo Hemorrhagic Fever: Tick-Host-Virus Interactions,” *Front. Cell. Infect. Microbiol.*, vol. 7, p. 213, 2017.

[32] R. Rodrigues, G. Paranhos-Baccalà, G. Vernet, and C. N. Peyrefitte, “Crimean-Congo

Hemorrhagic Fever Virus-Infected Hepatocytes Induce ER-Stress and Apoptosis Crosstalk," *PLoS One*, vol. 7, no. 1, p. e29712, Jan. 2012.

[33] R. Hewson, J. Chamberlain, V. Mioulet, G. Lloyd, B. Jamil, R. Hasan, A. Gmyl, L. Gmyl, S. E. Smirnova, A. Lukashev, G. Karganova, and C. Clegg, "Crimean-Congo haemorrhagic fever virus: Sequence analysis of the small RNA segments from a collection of viruses world wide," *Virus Res.*, vol. 102, no. 2, pp. 185–189, 2004.

[34] a Pekosz, J. Phillips, D. Pleasure, D. Merry, and F. Gonzalez-Scarano, "Induction of apoptosis by La Crosse virus infection and role of neuronal differentiation and human bcl-2 expression in its prevention.," *J. Virol.*, vol. 70, no. 8, pp. 5329–5335, 1996.

[35] D. Hacker, R. Raju, and D. Kolakofsky, "La Crosse virus nucleocapsid protein controls its own synthesis in mosquito cells by encapsidating its mRNA.," *J. Virol.*, vol. 63, no. 12, pp. 5166–5174, 1989.

[36] S. E. Newton, N. J. Short, and L. Dalgarno, "Bunyamwera virus replication in cultured Aedes albopictus (mosquito) cells: establishment of a persistent viral infection.," *J. Virol.*, vol. 38, no. 3, pp. 1015–1024, 1981.

[37] O. P. Zhirnov and V. V Syrtzev, "Influenza virus pathogenicity is determined by caspase cleavage motifs located in the viral proteins," *J Mol Genet Med*, vol. 3, no. 1, pp. 124–132, 2009.

[38] Y. Wang, S. Dutta, H. Karlberg, S. Devignot, F. Weber, Q. Hao, Y. J. Tan, A. Mirazimi, and M. Kotaka, "Structure of Crimean-Congo Hemorrhagic Fever Virus Nucleoprotein: Superhelical Homo-Oligomers and the Role of Caspase-3 Cleavage," *J. Virol.*, vol. 86, no. 22, pp. 12294–12303, 2012.

FIGURE LEGENDS

Figure 1. HAZV induces apoptosis in mammalian cells, A) Activation of apoptosis-associated caspases. SW13 cells were infected (Inf) with WT HAZV at a MOI of 1, alongside mock uninfected controls. At 24, 48 and 72 hours post infection lysates were collected and analysed via SDS-PAGE and western blotting using antibodies specific for the stated caspases (Casp), poly ADP-ribose polymerase (PARP), their cleaved forms (– C). Detection of GAPDH was used as a lysate loading control. B) Detection of dsDNA fragmentation associated with apoptosis. SW13 cells were infected with WT HAZV at an MOI of 1, alongside mock uninfected controls. At 24, 48 and 72 hours post infection, cells were visualized via confocal microscopy to identify nuclei displaying DNA fragmentation. Associated levels of TUNEL positive cells were determined relative to total cell number and displayed graphically (right).

Figure 2. Cleavage of HAZV-N in mammalian cells, A) Detection of multiple HAZV-N products. SW13 cells were infected with WT HAZV at an MOI of 1, and after 48 h, cell lysates were collected and analysed via SDS-PAGE and western blotting. Four species reactive to HAZV-N antisera were detected; full length N at 54 kDa, and cleavage products at 45 kDa (*), 30 kDa (**) and 20 kDa (***). Detection of GAPDH was used as a lysate loading control. B) Cleaved forms of HAZV-N were also detected in purified HAZV virions. C) Predicted caspase cleavage sites in HAZV-N determined by GraBCas prediction software, and the motifs with the three highest scores are displayed, with arrows indicating the site of cleavage. D) Representation of the predicted cleavage sites, NERD, DVMD and DQVD mapped onto the 3D structural model of HAZV-N. E) Schematic linear representation of the HAZV S-segment displaying relative locations of the NERD, DVMD and DQVD cleavage sites. Numbers correspond to amino acid positions within the HAZV-N ORF, non-translated regions (NTRs) are also shown.

Figure 3. Broad spectrum inhibition of caspases prevents HAZV-N cleavage. HAZV-N was progressively cleaved during the course of a 72 hour (hr) infection time course, with the ≈ 20 kDa cleavage product undetectable at A) 24 hours, and detectable with increasing abundance at B) 48 and, C) 72 hours post-infection. Detection of GAPDH was used as a lysate loading control in all blots. Inhibition of broad spectrum caspases with 20 μM or 40 μM Z-FA-FMK resulted in reduced detection of the ≈ 20 kDa band in comparison to the 0.1 and 0.2% DMSO controls. D) Cell viability in the presence of inhibitor and solvent was tested by treating cells with either 20 μM or 40 μM Z-FA-FMK, or cells 0.1% or 0.2% DMSO in triplicate. The graph represents an average of 3 independent absorbance readings.

Figure 4. The DQVD motif in HAZV-N is responsible for generation of cleavage products, and is cleaved by caspase 3. A) SW13 cells were transfected with either pCAGGS-HAZV-N or pCAGGS-HAZV-N(D272A) for 24 hours, then apoptosis was stimulated via treatment with 1 μM staurosporine (STS) for 4 hours. At this time point, total cell lysates were collected and analyzed for caspase 3 (Casp 3) its activated cleaved form (Casp 3 – C) and HAZV-N cleavage products via western blot. Detection of GAPDH was used as a lysate loading control. B) Tabulation of similar cleavage sites in related orthonairoviruses HAZV, CCHFV, Erve virus (ERVEV) and Dugbe virus (DUGV). C) Recombinant CCHFV and, D) HAZV-N proteins were digested overnight with recombinant cleaved caspase 3, and N specific products were identified by western blot analysis using CCHFV-N and HAZV-N antisera, respectively, revealing the generation of major cleavage products with molecular masses of approximately 20 and 30 kDa.

Figure 5. Differential activation of apoptosis and HAZV-N cleavage in SW13 and HAE/CTVM9 cells. A) Monolayers of SW13 or B) HAE/CTVM9 cells were infected with an HAZV at an MOI of 0.001. At the indicated time points post-infection, total cell lysates were collected and analyzed for HAZV-N expression by western blotting with HAZV-N antisera. C) Expression and activation of caspases (Casp) was determined by infection of monolayers of SW13 or HAE/CTVM9 cells with HAZV. Following infection, total cell lysates were collected at the indicated time points and probed for specific full length and cleaved (- C) forms of caspases. Detection of GAPDH was used as a lysate loading control. Actin and GAPDH were detected as lysate loading controls.

Figure 1

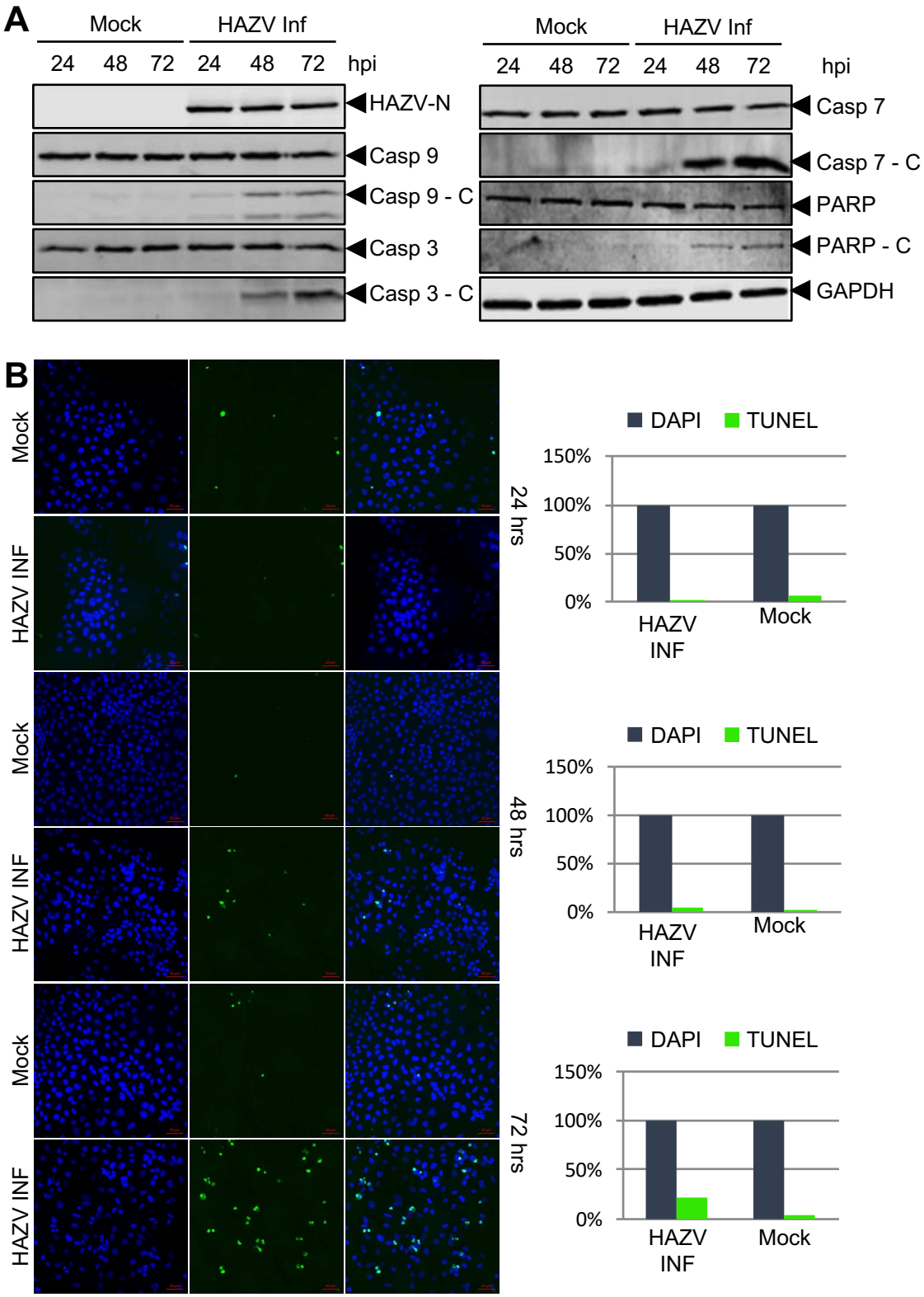
A
Mock
HAZV Inf
24 48 72 24 48 72 hpi
HAZV-N
Casp 9
Casp 9 - C
Casp 3
Casp 3 - C
Mock
HAZV Inf
24 48 72 24 48 72 hpi
Casp 7
Casp 7 - C
PARP
PARP - C
GAPDH
B
Mock
HAZV INF
Mock
HAZV INF
Mock
HAZV INF
24 hrs
48 hrs
72 hrs
DAPI
TUNEL
150%
100%
50%
0%
HAZV INF
Mock

Figure 2

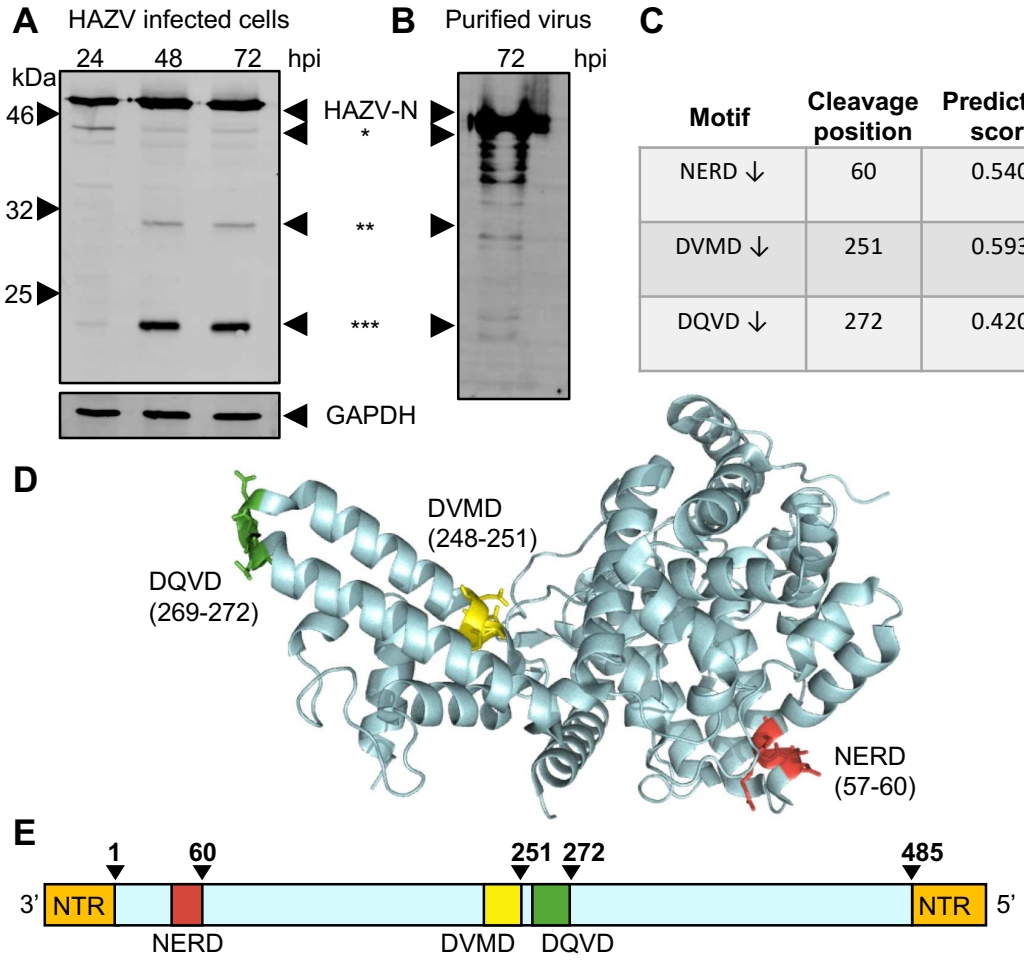
A
HAZV infected cells
24
48
72
hpi
kDa
46
32
25
HAZV-N
*
**
***
GAPDH
B
Purified virus
72
hpi
C
Motif
Cleavage position
Prediction score
NERD ↓
60
0.540
DVMD ↓
251
0.593
DQVD ↓
272
0.420
D
DVMD
(248-251)
DQVD
(269-272)
NERD
(57-60)
E
1
60
251
272
485
3'
NTR
NTR
5'
NERD
DVMD
DQVD

Figure 3

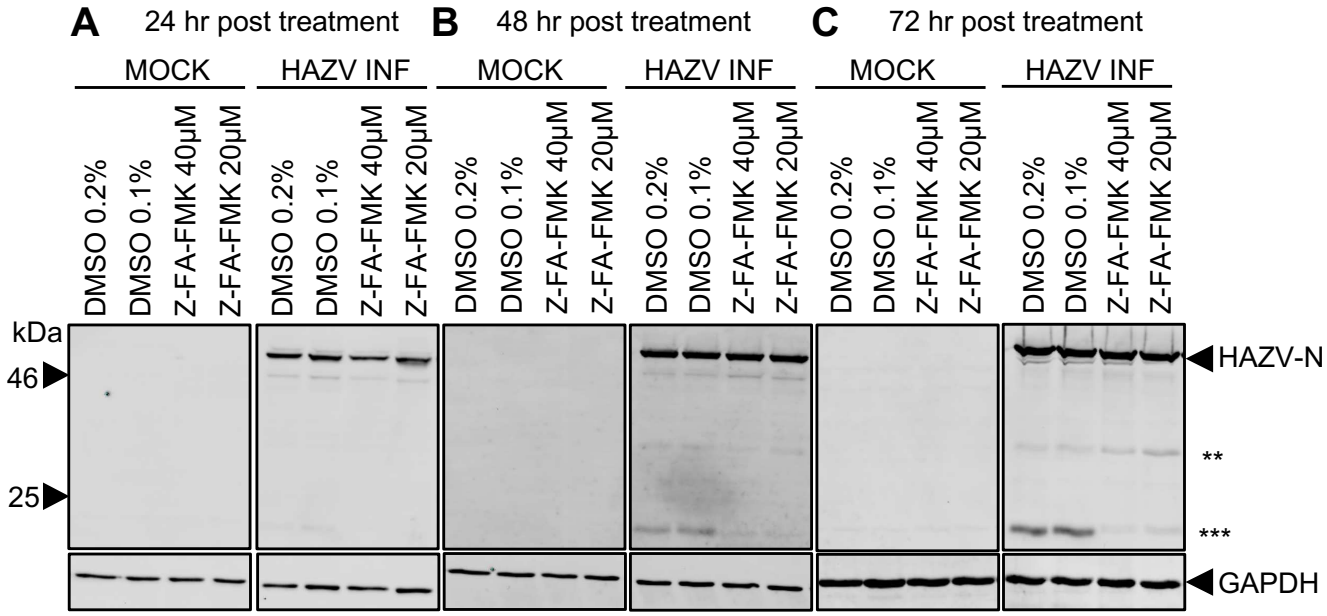
A
24 hr post treatment
B
48 hr post treatment
C
72 hr post treatment
MOCK
HAZV INF
MOCK
HAZV INF
MOCK
HAZV INF
DMSO 0.2%
DMSO 0.1%
Z-FA-FMK 40μM
Z-FA-FMK 20μM
kDa
46
25
HAZV-N
**
***
GAPDH

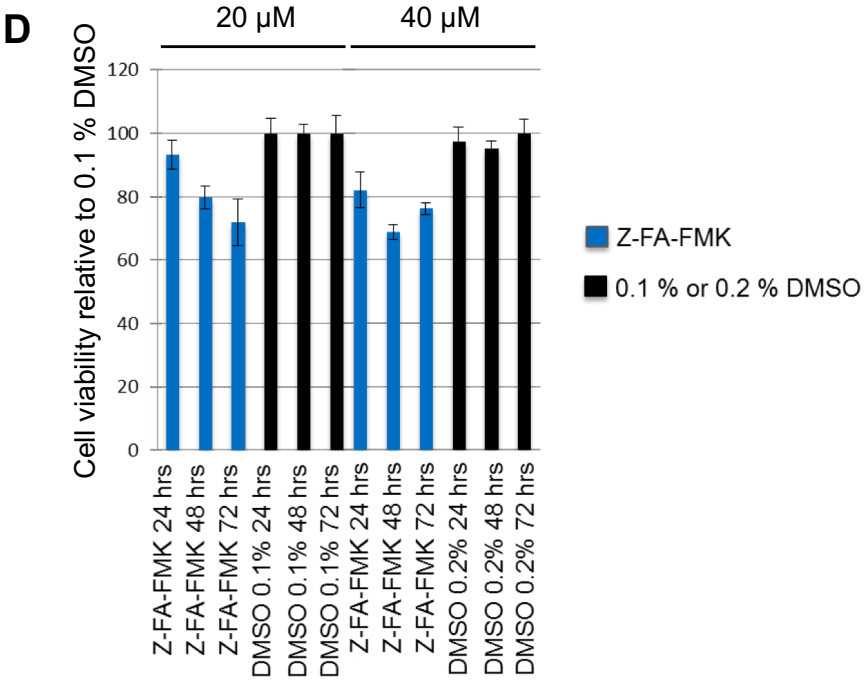
D
20 μM
40 μM
Cell viability relative to 0.1 % DMSO
120
100
80
60
40
20
0
Z-FA-FMK 24 hrs
Z-FA-FMK 48 hrs
Z-FA-FMK 72 hrs
DMSO 0.1% 24 hrs
DMSO 0.1% 48 hrs
DMSO 0.1% 72 hrs
Z-FA-FMK 24 hrs
Z-FA-FMK 48 hrs
Z-FA-FMK 72 hrs
DMSO 0.2% 24 hrs
DMSO 0.2% 48 hrs
DMSO 0.2% 72 hrs
Z-FA-FMK
0.1 % or 0.2 % DMSO

Figure 4

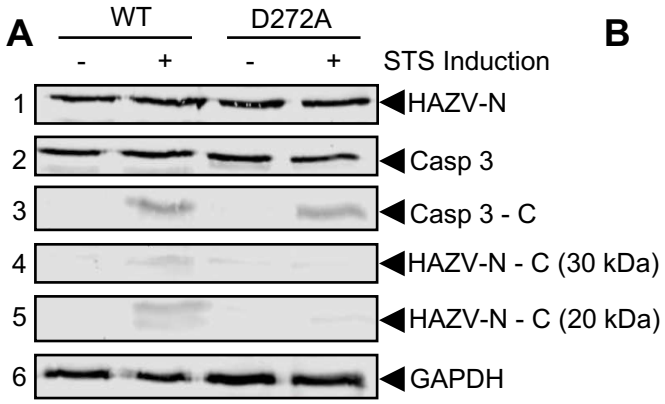

B

Virus	P1 position	Motif
HAZV	272	DQVD
CCHFV	269	DEVD
ERVEV	264	DVLD
DUGV	272	DQLD

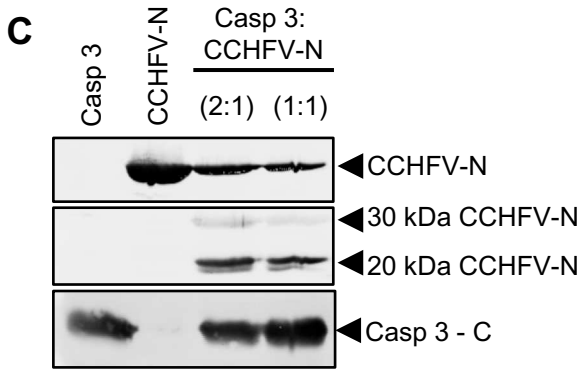

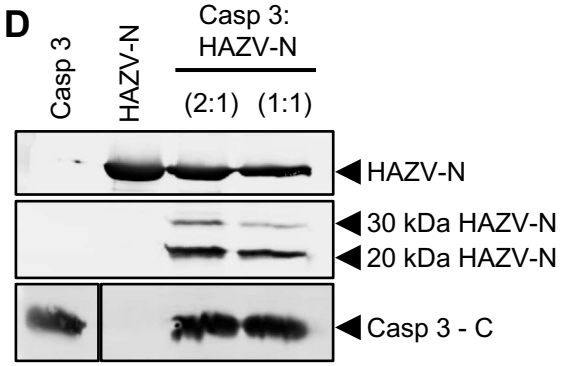

Figure 5

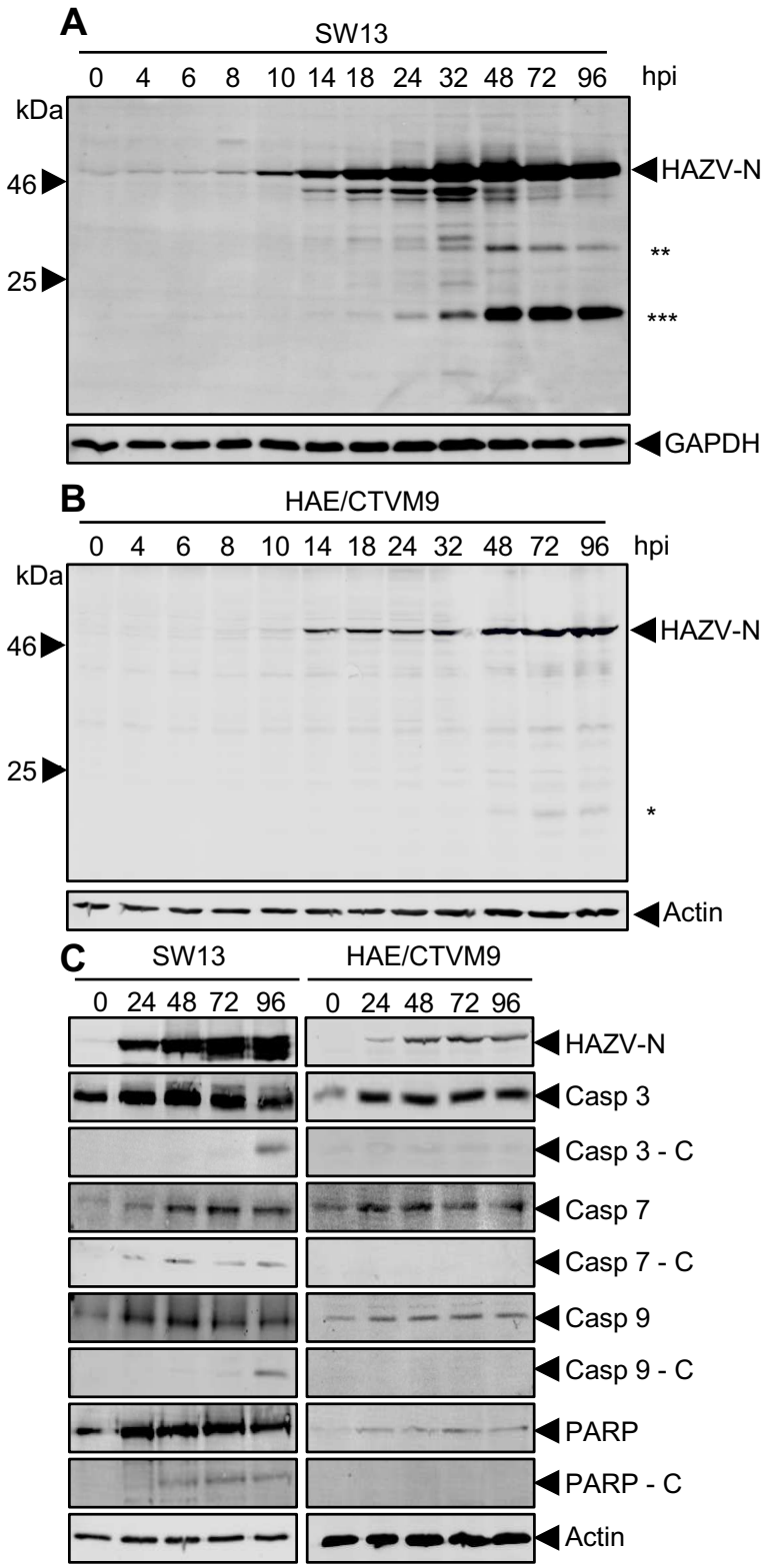
A
SW13
0 4 6 8 10 14 18 24 32 48 72 96 hpi
kDa
46
25
HAZV-N
**
***
GAPDH
B
HAE/CTVM9
0 4 6 8 10 14 18 24 32 48 72 96 hpi
kDa
46
25
HAZV-N
*
Actin
C
SW13
HAE/CTVM9
0 24 48 72 96
0 24 48 72 96
HAZV-N
Casp 3
Casp 3 - C
Casp 7
Casp 7 - C
Casp 9
Casp 9 - C
PARP
PARP - C
Actin